

Few Atom Detection and Manipulation Using Optical Nanofibres

Kieran Deasy^{1,2}, Amy Watkins^{2,3}, Michael Morrissey^{1,2,*}, Regine Schmidt³,
and Síle Nic Chormaic^{2,3}

¹Dept. Applied Physics and Instrumentation, Cork Institute of Technology, Bishopstown,
Cork, Ireland

²Physics Department, University College Cork, Cork, Ireland

³Photonics Centre, Tyndall National Institute, University College Cork,
Prospect Row, Cork, Ireland

{kieran.deasy, amy.watkins, regine.schmidt,
sile.nicchormaic}@tyndall.ie

Abstract. We study the coupling of spontaneously emitted photons from laser-cooled ^{85}Rb atoms to the guided modes of an optical nanofibre to demonstrate the potential such fibres offer as tools for detecting and manipulating cold atoms, even when the number of atoms is very small. We also demonstrate the integration of an optical nanofibre into an absorption spectroscopy setup, showcasing the ability of the evanescent field around nanofibres to interact with atoms in close proximity to the fibre. In principle, trapping of single atoms in engineered optical potentials on the surface of the fibre should facilitate entanglement between distant atoms mediated via the guided modes of the nanofibre.

Keywords: Atom fluorescence, optical nanofibres, evanescent field.

1 Introduction

The significance of single-mode and multimode optical fibres in classical data communications cannot be disputed. Single-mode silica optical fibre forms the backbone of many recent advances in classical data transfer over long distances. It seems inevitable that the functionality of optical fibres in quantum systems and quantum communication schemes should also come to a fore. In recent years, a number of methods for trapping and guiding cold, neutral atoms outside subwavelength optical fibres, i.e. optical nanofibres, has been proposed [1,2]. The strong interest in such techniques stems from the opportunities that arise in quantum information technologies and in studying atom-surface interactions. In order to fully predict the processes involved when a cold atom is close to the surface of an optical nanofibre, a thorough understanding of the spontaneous emission rate of atoms located near the fibre surface is crucial. Earlier theoretical [3] and experimental [4] work shows that the spectral distribution of atomic fluorescence is affected by the presence of the fibre, due to

* Current address: IESL, FORTH, P.O. Box 1527, Gr-711 10 Heraklion, Greece.

surface interactions resulting in a shift to the atomic transition frequency. In this work, we study the coupling of the spontaneous emission from laser-cooled rubidium atoms to the guided modes of an optical nanofibre to demonstrate the potential such fibres offer as tools for detecting and manipulating cold atoms, even when the number of atoms is very small [5].

As an alternative approach, light can be made propagate through an optical nanofibre, resulting in an intense evanescent field exponentially decaying from the surface of the fibre into the surrounding environment. This phenomenon has been theoretically studied extensively [6,7] and the evanescent light field has applications across a range of areas, in particular as an efficient method for coupling light into whispering gallery mode optical microcavities [8,9]. The evanescent field has also been used as an effective method for investigating the interaction of light and matter, for example in electromagnetically induced transparency (EIT) [10]. Nanofibres present a great opportunity to observe these interactions, providing a dual functionality of both supplying and collecting the probing light. In this work, we demonstrate the use of an optical nanofibre through which light is propagating in order to carry out absorption spectroscopy in a rubidium vapour cell. The interaction between the atoms and the light in the evanescent field yields an absorption signal that can be monitored at one end of the fibre. Currently, the Doppler-broadened peaks of the rubidium spectrum only are visible since a single beam pass has been used through the fibre.

2 Experimental Details and Results

In the work reported, there are two distinct experimental setups being used: one involves the integration of optical nanofibres as passive probes into a cloud of cold ^{85}Rb atoms and the other is the incorporation of an optical nanofibre, through which a very weak pump beam is passing, as an active probe into a Rb vapour cell. The fabrication and characterization of optical nanofibres is briefly described in section 2.1. The cold atom setup is described in section 2.2 and results demonstrating the coupling of spontaneously emitted photons from the laser-cooled atoms into the guided mode of a nanofibre are presented. This provides a unique tool for characterizing the properties of the magneto-optical trap (MOT). In section 2.3 we give details on the incorporation of the optical nanofibre into a Rb vapour cell setup where the eventual aim is to perform saturated absorption spectroscopy using the nanofibre.

2.1 Optical Nanofibres

Optical nanofibres are central to the two different experiments described here and the fabrication of the nanofibres is critical to the success of this work. A schematic diagram of the structure of an optical nanofibre is shown in Figure 1. The fabrication of optical nanofibres is based on heating and pulling a section of standard single mode fibre while ensuring that transmission through the fibre is high. From Figure 1 it can be seen that the fibres go through a transition region from being normal single mode fibre, where light is guided by the core/cladding refractive index difference, to a situation where the core has become negligible in the waist region of the nanofibre and the light is guided by the cladding/vacuum refractive index difference. When light is

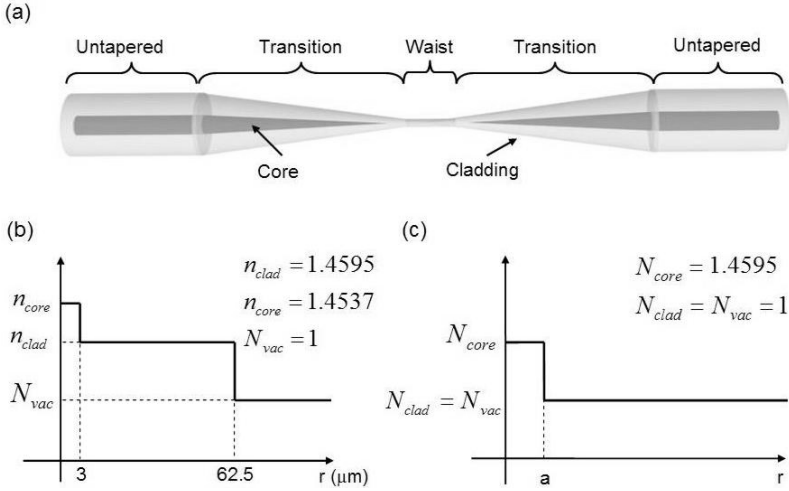


Fig. 1. (a) Diagram of the nanofibre. (b) Refractive index profile of ordinary single mode fibre. (c) Refractive index profile of the nanofibre in the waist region.

guided through the fibre a portion of it will be guided by the evanescent field at the waist region, external to the fibre, and this property is used when studying light-matter interactions with nanofibres. Alternatively, light can also be efficiently coupled into the fibre at the waist region and this property has been exploited by surrounding the fibre with cold atoms and monitoring the spontaneous emission from the atoms into the fibre's guided modes.

There are a number of techniques used for fabricating optical nanofibres [11] and we employ a standard heat and pull technique similar to that described elsewhere [12]. Within a clean environment, stripped, commercially available single-mode fibre is heated using an oxy-butane flame and then the two ends of the fibre are simultaneously drawn apart in opposite directions using a pair of stepper motors while monitoring the fibre transmission. Due to this extension the volume of the fibre within the hot zone is reduced, consequently reducing the fibre diameter [13]. The fibre diameter after the pulling process is a function of both the pull length and the length of the hot zone according to the adiabatic condition [14]. The oxygen-butane mixture is carefully selected to ensure a clean burning flame, eliminating any contaminants which may otherwise be deposited on the fibre, thereby reducing its transmission. A schematic of the pulling rig is shown in Figure 2. Using this design, nanofibres with a diameter of less than 1 μm and a transmission at 780 nm of over 90% are routinely produced.

2.2 Cold Atom Setup

For these experiments a cloud of cold ^{85}Rb atoms is produced using a standard MOT setup [15]. The cooling laser is locked 12 MHz red detuned from the $5S_{1/2}$, $F=3 \rightarrow 5S_{3/2}$, $F'=4$ transition using saturated absorption spectroscopy (SAS). The repump

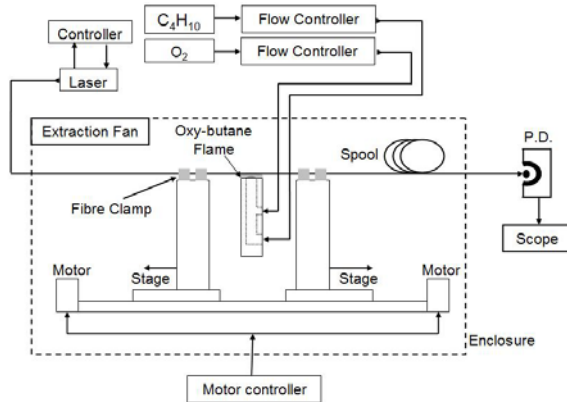


Fig. 2. Schematic diagram of the heat-and-pull rig used to fabricate the optical nanofibres

laser is also locked using SAS to the $5S_{1/2}$, $F=2 \rightarrow 5S_{3/2}$, $F'=3$ transition. Three orthogonal counter-propagating cooling beams intersect with the repumper beam and the zero of an inhomogeneous magnetic field with a field gradient of 10 G/cm at the centre of an octagonal vacuum chamber. Rubidium is supplied into the chamber using resistively heated dispensers, allowing the background Rb vapour to be controlled via the dispenser current.

The nanofibre is mounted on a U-mount and installed vertically into the chamber. The UHV is maintained by feeding the fibre into the chamber through a Teflon ferrule held in place using a Swagelok. The nanofibre is positioned in a manner to ensure the waist is overlapped by the cloud of cold atoms. The fibre we use for this work has a diameter of ~ 600 nm and a transmission of 85% at 780 nm after fabrication. Small changes to the MOT position can be made by the manipulation of magnetic fields using external coils. This ensures a good overlap of the MOT and the waist region of the fibre, as shown in Figure 3(a). Note that two fibres were installed in the UHV system but the results are all taken using a single fibre (TONF 1).

To monitor the position of the atom cloud a number of CCD cameras are placed around the chamber to provide viewing from all directions. This is to ensure that the overlap is excellent, thereby guaranteeing efficient coupling of spontaneously emitted photons from the atoms into the guided modes of the nanofibre as illustrated in Figure 3(b). The photon count rate is detected at one fibre end using a single photon counting module (SPCM, PerkinElmer, SPC-AQRH-14-FC) connected to a counter (Hamamatsu Counting Unit, C8855). It is also important to compare results obtained using the nanofibre probe with those taken using a more conventional method for analyzing MOT characteristics, such as loading time and lifetime. For this purpose, a fluorescence detection scheme was incorporated, whereby fluorescence from the MOT was focused onto a photodiode using a series of lenses. The signal yields information concerning the number of trapped atoms in the MOT. A schematic of the fluorescence detection scheme is shown in Figure 4.

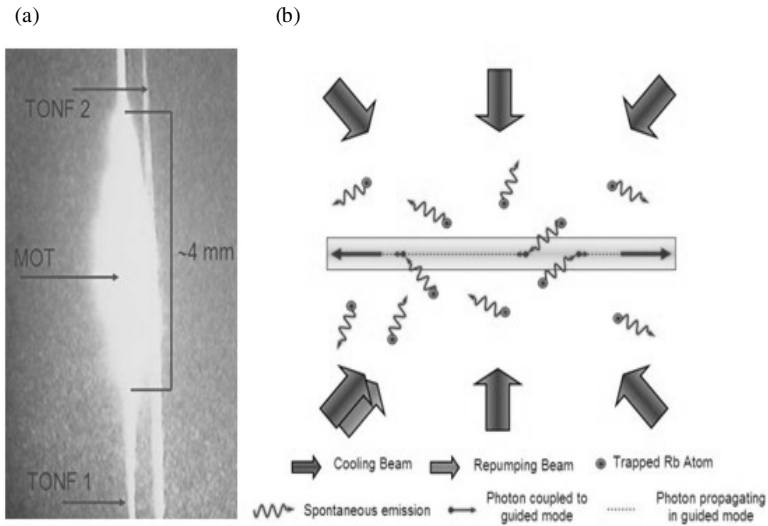


Fig. 3. (a) CCD image of the cloud of laser-cooled ^{85}Rb atoms overlapping the nanofibre. (b) Schematic of the atom cloud overlapping the nanofibre. Spontaneously emitted photons are detected at one end of the fibre.

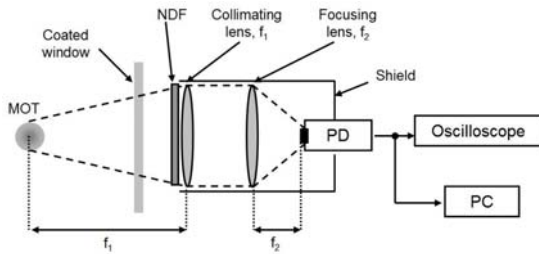


Fig. 4. Schematic diagram of the fluorescence detection system. PD: photodiode, NDF: neutral density filter, PC: personal computer.

2.2.1 Photon Coupling

Efficient coupling of fluorescence photons from the cold atoms into the guided modes of the nanofibre are critical for this work. The first measurement was an analysis of the efficiency of the photon coupling into the nanofibre. Initially, the cooling laser, repumper and anti-Helmholtz coils were switched off to determine the background count rate on the detector. The repump laser was then switched on, followed by the cooling laser and finally the anti-Helmholtz coils were switched on and the cold atom cloud was formed. The components were then switched off in the reverse order. The signal recorded on the single photon counter is shown in Figure 5. From these results, it is clear that the increase in signal obtained when the anti-Helmholtz coils are switched on is significant and this dramatic change in count rate of approximately $4 \times 10^5 \text{ s}^{-1}$ is attributed to fluorescence from the trapped atoms.

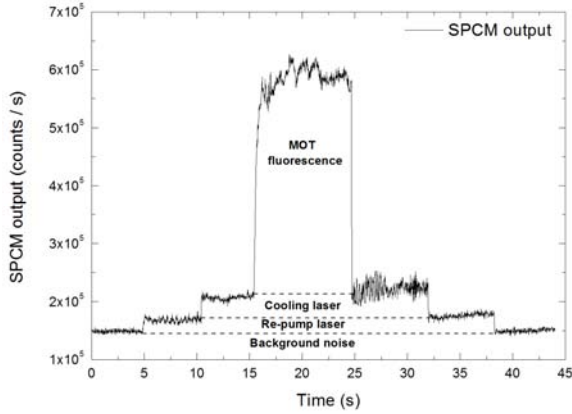


Fig. 5. Coupling of photons into the optical nanofibre from a cloud of ^{85}Rb atoms

To verify this result the photon count rate, η_p , can be determined from:

$$\eta_p = N_{\text{eff}} \eta_f \gamma_{sc} \eta_D T, \quad (1)$$

where N_{eff} is the effective number of atoms, η_f is the coupling efficiency of spontaneously emitted photons into the guided modes of the fibre, η_D is the quantum efficiency of the detector at 780 nm, and T is the transmission through the fibre. The effective number of atoms is the number of atoms contributing to the spontaneous emission signal and this is calculated by considering a 2 mm long hollow cylindrical volume extending 300 nm from the fibre surface and using the density of the MOT to determine the number of atoms in this region. Typically six atoms would be contained in this volume. Using the laser intensity and detuning of the cooling laser the atomic scattering rate can be determined as $\gamma_{sc} = 6.5 \times 10^5 \text{ s}^{-1}$. With these values we calculate the value for $\eta_p = 3.7 \times 10^5 \text{ s}^{-1}$, in good agreement with the experimental value observed.

2.2.2 Loading Time

The loading time is the $1/e$ time taken for the MOT to load with atoms once the magnetic field is switched on. The MOT is loaded from the background rubidium vapour. Here, we compare the results for the loading time taken from photons coupled into the nanofibre and detected at one end of the fibre on the SPCM for different Rb dispenser currents and these are shown in Figure 6. For comparison, the real-time loading evolution of the MOT as determined by focusing the emitted fluorescence from the atom cloud onto a photodiode (PD) is also shown. The Rb dispenser was turned on and allowed to stabilize for 15 minutes before the magnetic field was switched on. This was to remove any fluctuations due to variances in the Rb vapour pressure for a specific dispenser current. Loading times of ~ 0.5 s were obtained and both detection methods are in reasonably good agreement.

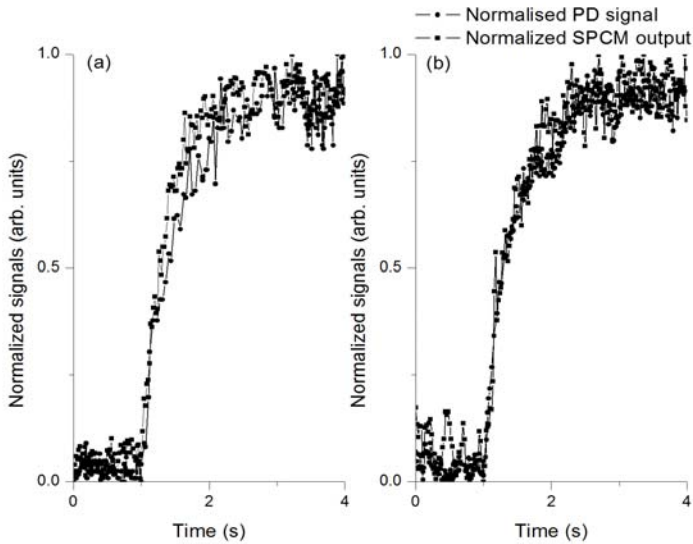


Fig. 6. Loading time of the MOT measured using a PD (*full circles*) and an optical nanofibre (*full squares*). (a) Getter current of 3.3 A, (b) Getter current of 3.7 A.

2.2.3 Lifetime

The lifetime of the MOT is the $1/e$ time it takes for the atoms to escape from the MOT once the Rb dispenser is switched off. At this point, the loss rate from the trap is greater than the capture rate and the lifetime is determined by measuring the decay the number of trapped atoms. Again, we compare results using fluorescence imaging onto a PD and fluorescence coupling into the nanofibre for two different getter currents and these are shown in Figure 7.

From Figure 7 (a) and (b) it can be seen that the value observed for the lifetime using the PD detection scheme is relatively consistent at 8 - 9 seconds. However, for the nanofibre probe the lifetime varies significantly depending on the getter current. It can be seen that there is a longer lifetime observed using the nanofibre probe compared to the PD signal and this is extended even further when higher getter currents are applied. Two possible explanations for this can be proposed: firstly atoms at the extremities of the atom cloud are hotter than those at the centre of the cloud and, therefore, are lost faster. This will have a greater effect on the fluorescence detected by the PD, which monitors the entire atom cloud as opposed to the nanofibre, which only detects signal from atoms at or near the centre. The second possible reason is due to sensitivity; the nanofibre is a very sensitive device capable of detecting fluorescence for a small number of atoms remaining in its vicinity. This shows a clear advantage for using the nanofibre as a probe in a low density MOT or for detecting few atoms as compared to standard photodiode imaging schemes.

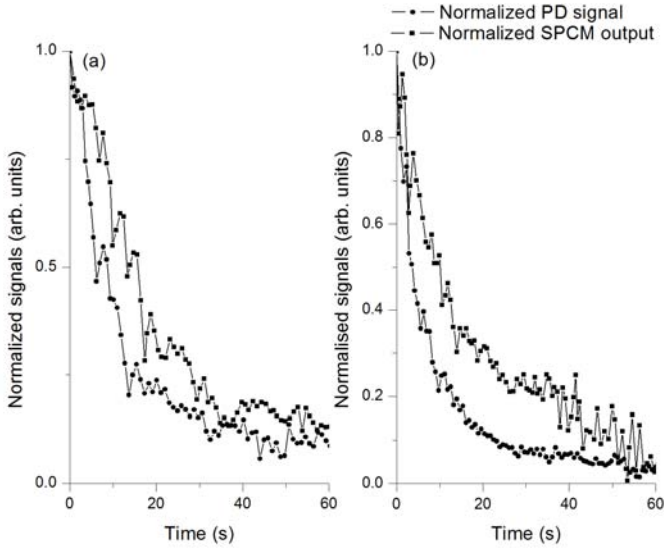


Fig. 7. Plots showing the lifetime of the MOT as taken using a PD (*full circles*) and using the nanofibre (*full squares*). (a) Getter current of 3.3 Amps, (b) Getter current of 3.7 Amps.

2.3 Rubidium Vapour Cell Setup

For this experiment a rubidium vapour cell is formed in a 4-way vacuum cross pumped down to 10^{-2} mbar using a roughing pump. A Rb dispenser in the chamber

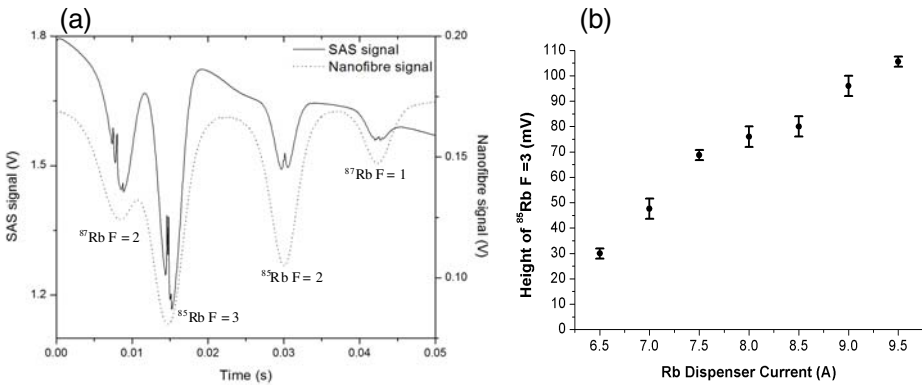


Fig. 8. (a) Absorption signal (*dashed line*) through the optical nanofibre for the D2 lines in ^{85}Rb and ^{87}Rb . For comparison the saturated absorption signal (*solid line*) using a standard setup is also shown. Fibre transmission $\sim 2\%$. (b) Height of the ^{85}Rb F = 3 D2 line as a function of Rb dispenser current. Fibre transmission $\sim 5\%$.

provides both the ^{85}Rb and ^{87}Rb isotopes. An optical nanofibre is mounted on a U-mount and placed in the chamber using the same techniques as in the cold atom setup. A Toptica DL100 laser at around 780 nm is scanned across the Rb transitions and approximately 2 μW of power is coupled into the nanofibre, which has a very low transmission of $\sim 2\%$. The transmitted signal is monitored using a SensL Silicon Photomultiplier (SPM) Micro3000 Series 2 placed at one end of the fibre and is shown in Figure 8. As a comparison, the saturated absorption spectrum is also shown for the same laser. One can clearly see that the Doppler-broadened absorption dips are obtainable using this technique. In addition, the height of the ^{85}Rb $F = 3$ dip has been plotted as a function of current through the Rb dispenser and, as expected, it increases with increasing current. The next stage in this work will be the incorporation of a probe beam in order to obtain a saturated absorption signal through the nanofibre.

3 Conclusion

In conclusion, we have demonstrated the use of optical nanofibres as passive probes for cold atom samples and as active probes in a rubidium vapour cell. The nanofibre can be used to determine characteristics associated with the cloud of cold atoms, such as the lifetime and the loading time of the MOT as a function of background vapour pressure. The loading time measurements compare favourably with those made using conventional imaging techniques. However, the lifetime measurements differ significantly for both techniques. This is likely due to the MOT switching from the temperature limited regime to the constant density regime. In order to study this effect in more detail, future work will concentrate on symmetrizing the profile of the atom cloud and increasing MOT loading times by reducing the amount of rubidium dispensed into the vacuum chamber.

We have also observed absorption of the light field through an optical nanofibre when placed in a Rb vapour cell. An initial, Doppler-broadened spectrum has been observed with less than 2 μW of power coupled into the fibre and a very low fibre transmission of 2%. This shows the sensitivity afforded by using optical nanofibres as active probes. The next stage in this work will consist in incorporating a probe beam into the vapour cell in order to observe the saturated absorption spectrum.

Acknowledgments. This work is supported by Science Foundation Ireland under Grant No. 07/RFP/PHYF518 and the HEA through the INSPIRE programme. K.D. and A.W. acknowledge support from IRCSET through the Embark Initiative. R.S. acknowledges support from the ESF CASIMIR research networking programme.

References

1. Le Kien, F., Balykin, V.I., Hakuta, K.: Atom trap and waveguide using a two-color evanescent light field around a subwavelength-diameter optical fiber. *Phys. Rev. A* 70, 063403 (2004)
2. Sagué, G., Baade, A., Rauschenbeutel, A.: Blue-detuned evanescent field surface traps for neutral atoms based on mode interference in ultra-thin optical fibres. *New J. Phys.* 10, 113008 (2008)

3. Russell, L., Gleeson, D.A., Minogin, V.G., Nic Chormaic, S.: Spectral distribution of atomic fluorescence coupled into an optical nanofibre. *J. Phys. B* 42, 185006 (2009)
4. Nayak, K.P., Melentiev, P.N., Moringa, M., Le Kien, F., Balykin, V.I., Hakuta, K.: Optical nanofiber as an efficient tool for manipulating and probing atomic fluorescence. *Optics Express* 15, 5431 (2007)
5. Morrissey, M.J., Deasy, K., Wu, Y., Chakrabarti, S., Nic Chormaic, S.: Tapered optical fibers as tools for probing magneto-optical trap characteristics. *Rev. Sci. Instrum.* 80, 053102 (2009)
6. Bures, J., Ghosh, R.: Power density in the vicinity of a tapered fiber. *J. Opt. Soc. Am. A* 16, 1992 (1999)
7. Tong, L., Lou, J., Mazur, E.: Single-mode guiding properties of subwavelength-diameter silica and silicon wire waveguides. *Optics Express* 12, 1025–1035 (2004)
8. Cai, M., Painter, O., Vahala, K.J.: Observation of critical coupling in a fiber taper to a silica-microsphere whispering-gallery mode system. *Phys. Rev. Lett.* 85, 74–77 (2000)
9. Ward, J.M., Féron, P., Nic Chormaic, S.: A taper-fused microspherical laser source. *IEEE Photonics Technology Letters* 20, 392–394 (2008)
10. Spillane, S.M., Pati, G.S., Salit, K., Hall, M., Kumar, P., Beausoleil, R.G., Shahriar, M.S.: Observation of nonlinear optical interactions of ultralow levels of light in a tapered optical nanofiber embedded in a hot rubidium vapor. *Phys. Rev. Lett.* 100, 233602 (2008)
11. Tong, L., Gattass, R.R., Ashcom, J.B., He, S., Lou, J., Shen, M., Maxwell, I., Mazur, E.: Subwavelength-diameter silica wires for low-loss optical wave guiding. *Nature* 426, 816–819 (2003)
12. Ward, J.M., O’Shea, D.G., Shortt, B.J., Morrissey, M.J., Deasy, K., Nic Chormaic, S.: Heat-and-pull rig for fiber taper fabrication. *Rev. Sci. Instrum.* 77, 083105 (2006)
13. Birks, T., Li, Y.: The shape of fiber tapers. *J. Light. Tech.* 10, 432 (1992)
14. Love, J.D., Henry, W.M., Stewart, W.J., Black, R.J., Lacroix, S., Gonthier, F.: Tapered single-mode fibres and devices. 1. Adiabaticity criteria. *IEEE Proc.* 138, 342 (1991)
15. Metcalf, H.J., van der Straten, P.: *Laser Cooling and Trapping*. Springer, Heidelberg (1999)